Electronic Supplementary Information

Exploring the symbol processing 'time interval' parametric constraint in a Belousov-Zhabotinsky operated chemical Turing Machine

Thomas C. Draper,[a] Marta Dueñas-Díez,[ab] and Juan Pérez-Mercader[ac]

[a] Department of Earth and Planetary Sciences and Origins of Life Initiative, Harvard University, Cambridge, Massachusetts, 02138-1204, United States

[b] Repsol Technology Lab, c/ Agustín de Betancourt, s/n., 28935, Móstoles, Madrid, Spain

[c] Santa Fe Institute, Santa Fe, New Mexico, 87501, United States

Variability in the Induction Period

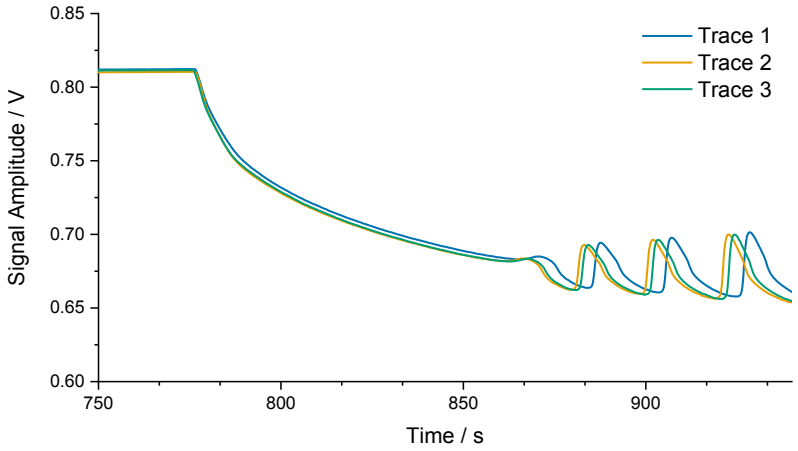

Figure S1: Replicate experimental runs typically show a high degree of reproducibility. However slight variation can occur as demonstrated here, where one of the experimental traces is shown to be out-of-sync with the other traces. All three of these experiments were run using the Opentrons OT-2 automatic pipetting robot. These traces are all for the word $a^2b^2c^3$, with τ=250 s.

The length of the induction period, the stage post-addition of the first malonic acid aliquot (b_1), can vary by up to 5 seconds (in 90 seconds) between replicate runs (see figure S1). The induction period in the BZ reaction is a consequence of the finite time required for a sufficient concentration of brominated malonic acid to accumulate in the reaction vessel. It has previously been shown that the induction period decreases exponentially as bromide anion concentration increases,[1] suggesting that it is very sensitive to changes. In our experiments, no bromide anion is directly added (unlike others),[2,3] instead, it is formed *in situ* through the cascading reactions, initially between sodium bromate and the metal catalyst.[4] Whilst all the bromine in our reaction vessel comes from a single molecular source, it has many different reaction paths available to it, before it is able to react with the malonic acid. The inherent natural variation, such as Brownian motion, would cause slight differences in the occupation of each of these paths, each of which would have different activation energies and rate constants. Consequently, the time point whereby a critical amount of bromide is formed will fluctuate slightly, which in turn has an exponential effect on the length of the induction period.

Peaks in Measurement Zone

The number of oscillations in the measurement zone is directly related to the time interval for a given word and the number of aliquots (i.e. the concentration) of sodium bromate 'a' in the reaction (see figure S2(a)). Malonic acid 'b' and sodium hydroxide 'c' also have an effect, but to a lesser extent. The sodium bromate has a stronger effect because it can directly involve itself in the redox cycle immediately, whereas the first steps of the malonic acid require its bromination, which is a comparatively slow reaction.[4] Additionally, each aliquot of sodium bromate contains a greater molar quantity than the other aliquots (2.00 mmol of $NaBrO_3$, compared to 0.875 mmol of malonic acid, and 1.25 mmol of NaOH).

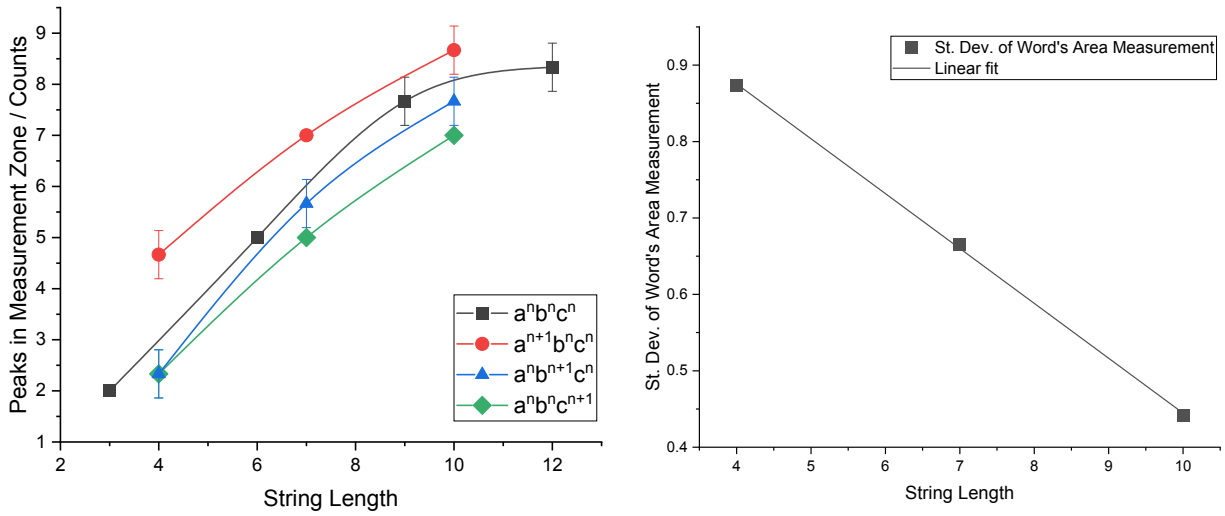

Figure S2: (a) The average number of oscillation peaks in the measurement zone increases as the word length increases. This is primarily due to the increase in the concentration of sodium bromate. Note the number of peaks in the measurement zone positively correlates with the oscillation frequency. All points have error bars, which are standard deviations. (b) For words $a^{n+1}b^nc^n$, the longer the string length, the smaller the absolute standard deviation of the Area metric. $R^2 = 1.000$. All $\tau = 250$ s.

This stronger effect of the sodium bromate is also visible in figure S2(b), where there is a clear inverse correlation between the absolute standard deviation of the Area measurements and the length of the word in form: $a^{n+1}b^nc^n$. This is again due to the extra sensitivity that this recipe of the BZ reaction has to changes in the concentration of sodium bromate caused by additional aliquots. As the word length increases, the number of peaks in the measurement zone increases, and the relative standard deviation decreases.

Distance-Frequency Plots

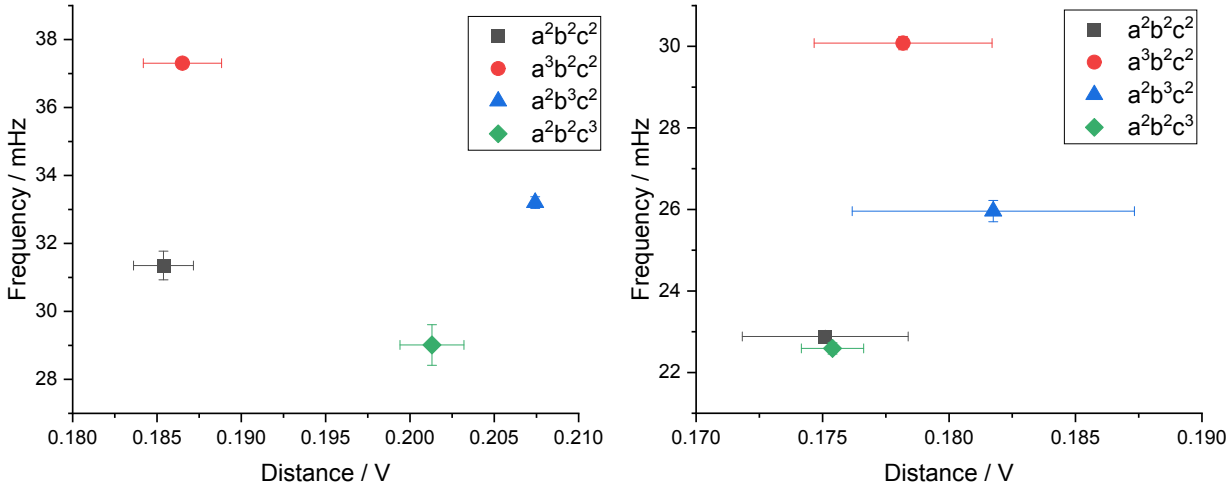

Figure S3: Distance-Frequency plots for both (a) $\tau = 450$ s, and (b) $\tau = 250$ s. Note the much greater varience in the Distance measurements when $\tau = 250$ s.

Statistical Analysis of Area Measurements when τ = 450 s

Table S1: Results from Levene's Test of the homogeneity of variances, for Area measurements taken when the time interval is 450 s.

	Levene Statistic	df1	df2	Sig.
Based on Mean	0.391	3	8	0.763
Based on Median	0.059	3	8	0.980
Based on Median and with adjusted df	0.059	3	6.353	0.979
Based on trimmed mean	0.347	3	8	0.793

Table S2: Results from one-way analysis of variance (ANOVA), for Area measurements taken when the time interval is 450 s.

	Sum of Squares	df	Mean Square	F	Sig.	η^2
Between Groups	423.406	3	141.135	184.060	1.018E-07	0.986
Within Groups	6.134	8	0.767			
Total	429.540	11				

Table S3: Results from Tukey's HSD post-hoc test, for Area measurements taken when the time interval is 450 s.

Word (I)	Word (J)	Mean Difference (I-J)	Std. Error	Sig.
$a^2b^2c^2$	$a^2b^2c^3$	-6.97035	0.71498	0.000
	$a^2b^3c^2$	-12.07852	0.71498	0.000
	$a^3b^2c^2$	3.14508	0.71498	0.010
$a^2b^2c^3$	$a^2b^2c^2$	6.97035	0.71498	0.000
	$a^2b^3c^2$	-5.10817	0.71498	0.000
	$a^3b^2c^2$	10.11543	0.71498	0.000
$a^2b^3c^2$	$a^2b^2c^2$	12.07852	0.71498	0.000
	$a^2b^2c^3$	5.10817	0.71498	0.000
	$a^3b^2c^2$	15.22360	0.71498	0.000
$a^3b^2c^2$	$a^2b^2c^2$	-3.14508	0.71498	0.010
	$a^2b^2c^3$	-10.11543	0.71498	0.000
	$a^2b^3c^2$	-15.22360	0.71498	0.000

Statistical Analysis of Area Measurements when τ = 250 s

Table S4: Results from Levene's Test of the homogeneity of variances, for Area measurements taken when the time interval is 250 s.

	Levene Statistic	df1	df2	Sig.
Based on Mean	1.061	3	8	0.418
Based on Median	0.391	3	8	0.763
Based on Median and with adjusted df	0.391	3	6.336	0.764
Based on trimmed mean	1.001	3	8	0.441

Table S5: Results from one-way analysis of variance (ANOVA), for Area measurements taken when the time interval is 250 s.

	Sum of Squares	df	Mean Square	F	Sig.	η^2
Between Groups	13.895	3	4.632	6.777	0.014	0.718
Within Groups	5.467	8	0.683			
Total	19.362	11				

Table S6: Results from Tukey's HSD post-hoc test, for Area measurements taken when the time interval is 250 s.

Word (I)	Word (J)	Mean Difference (I-J)	Std. Error	Sig.
$a^2b^2c^2$	$a^2b^2c^3$	-0.83039	0.67497	0.627
	$a^2b^3c^2$	-2.12185	0.67497	0.054
	$a^3b^2c^2$	0.78416	0.67497	0.665
$a^2b^2c^3$	$a^2b^2c^2$	0.83039	0.67497	0.627
	$a^2b^3c^2$	-1.29146	0.67497	0.295
	$a^3b^2c^2$	1.61456	0.67497	0.156
$a^2b^3c^2$	$a^2b^2c^2$	2.12185	0.67497	0.054
	$a^2b^2c^3$	1.29146	0.67497	0.295
	$a^3b^2c^2$	2.90601	0.67497	0.011
$a^3b^2c^2$	$a^2b^2c^2$	-0.78416	0.67497	0.665
	$a^2b^2c^3$	-1.61456	0.67497	0.156
	$a^2b^3c^2$	-2.90601	0.67497	0.011

Plots of Experimental Voltage Traces

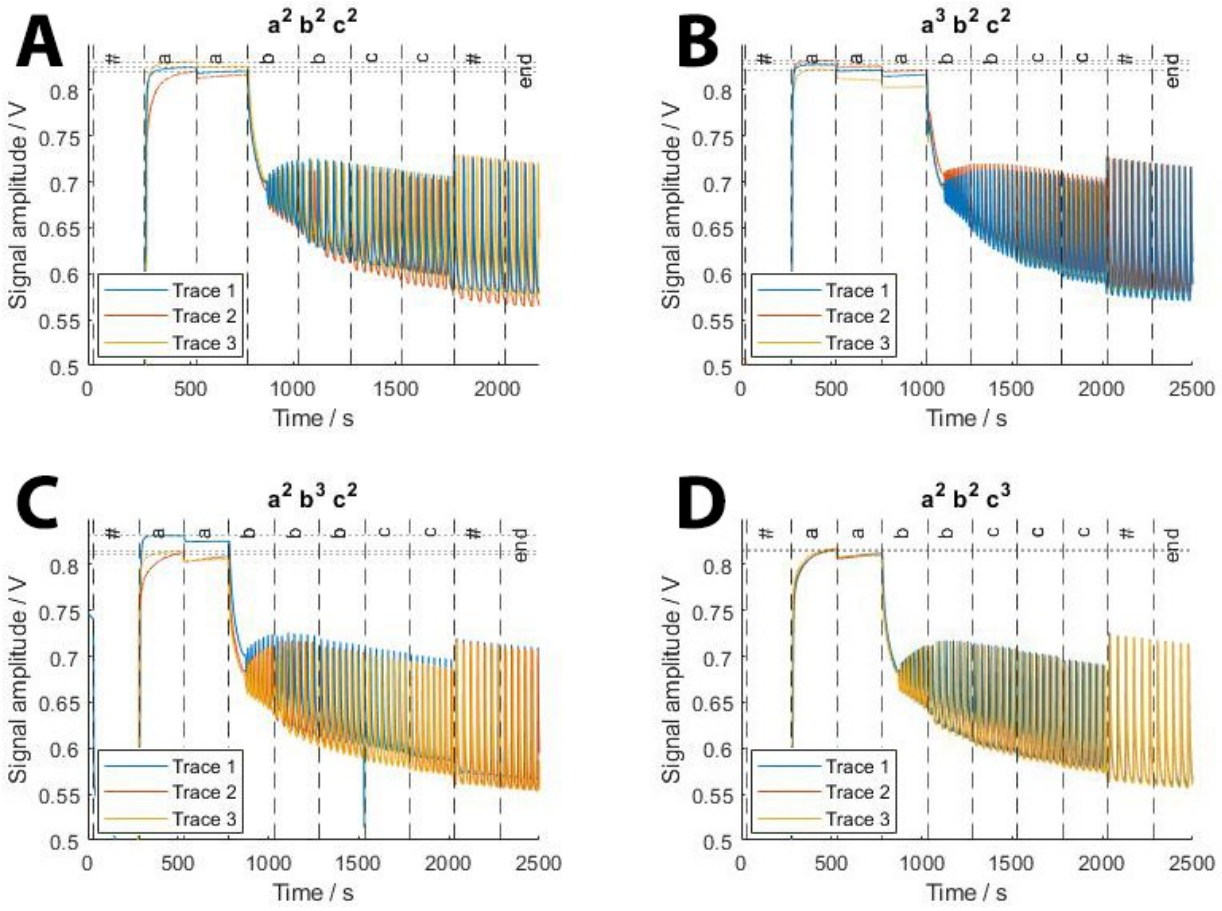

Figure S4: Experimental data for when τ = 250 s, for words (a) $a^2b^2c^2$, (b) $a^3b^2c^2$, (c) $a^2b^3c^2$, and (d) $a^2b^2c^3$. Each word has been run in triplicate and plotted over each other to demonstrate the reproducibility. Each blue, red, and orange trace represents a different experiment, with each word run in triplicate. Note the slight differences in the achieved values of V_{max}. All experiments were run using the Opentrons OT-2 automatic pipetting robot.

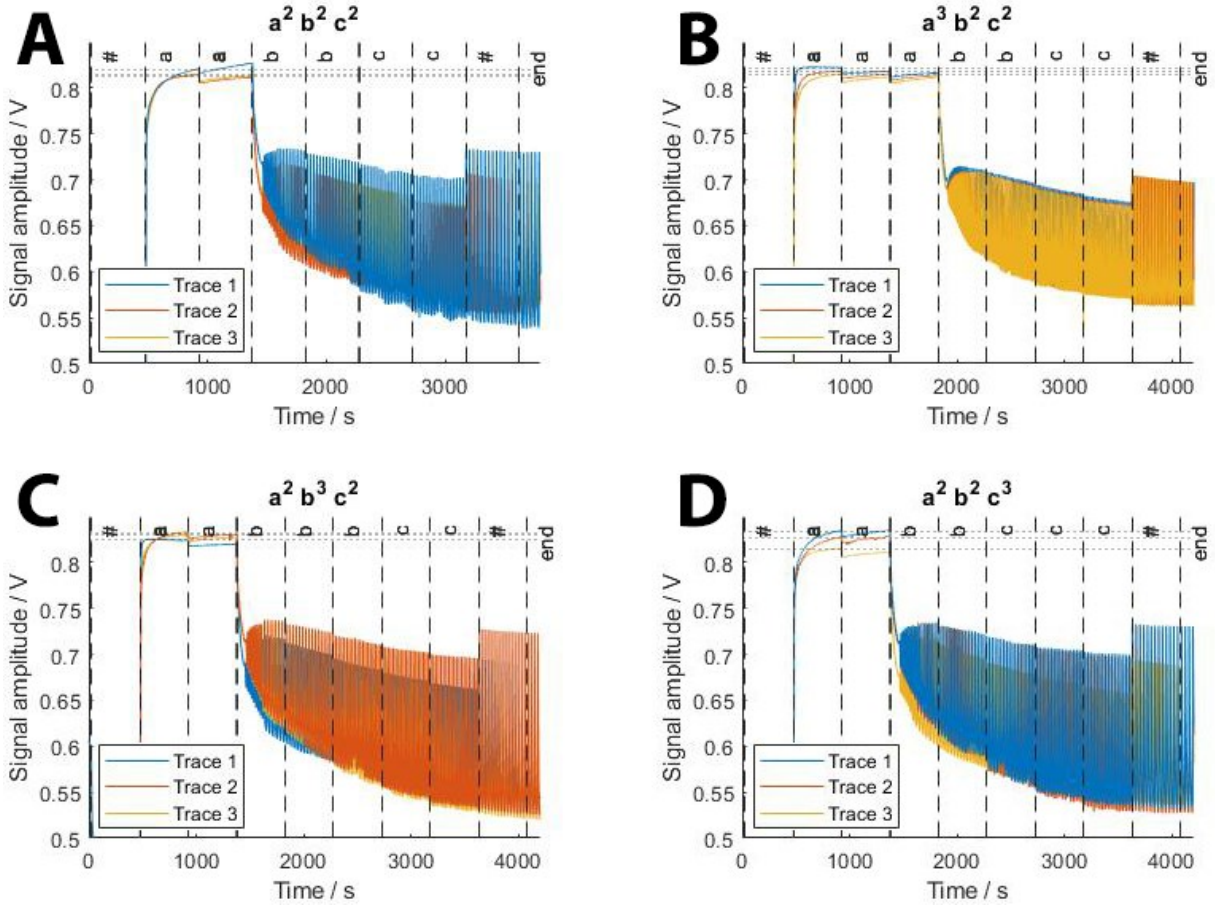

Figure S5: Experimental data for when $\tau = 450$ s, for words (a) $a^2b^2c^2$, (b) $a^3b^2c^2$, (c) $a^2b^3c^2$, and (d) $a^2b^2c^3$. Each word has been run in triplicate and plotted over each other to demonstrate the reproducibility. Each blue, red, and orange trace represents a different experiment, which each word run in triplicate. Note the slight differences in the achieved values of V_{max}. All experiments were run using the Opentrons OT-2 automatic pipetting robot.

Modified FKN kinetic Model Simulations

Kinetic simulations based on a representative model of the chemical reaction mechanism can greatly facilitate the design and implementation of native chemical automata, e.g. to specify the aliquots recipes and to optimize the ACCEPT/REJECT criterion.[5,6] Luckily, the kinetics of the Belousov-Zhabotinsky reaction have been widely studied over the years, and models of different levels of complexity are available. Here we chose a modified version of the well-known Field-Körös-Noyes kinetic mechanism,[4] described in detail in reference 5. Simpler models like the Oregonator[7] are not adequate since they do not describe the bromination and reduction of the organic subset in sufficient detail, while more advanced models like the Gao-Försterling[8] are too complex and would considerably slow down optimization.

The Field-Körös-Noyes kinetic mechanism was modified as reported in reference 5: inclusion of a kinetic equation for the bromination of bromomalonic acid into dibromomalonic acid, and of the complete acid-base neutralization of the NaOH aliquots. The latter is not included as a reaction per se, but as a (downwards) step change in the proton concentration any time a NaOH "c" aliquot is added to the reactor.

No further modification was needed to be able to simulate changes in the time interval, since the model was built in such a way that it simulates one symbol at a time for the duration of one time interval, stores the final values of the variables using them as initial conditions in the subsequent symbol until all symbols in the sequence are simulated. It is then implemented as a "for" loop with 3n+1 consecutive simulations of the ODE system for L_3. Hence, the time interval was already an input parameter of the simulation, and while before its value was always 450s, for this work we just had to change it to 250s without requiring modification of the code otherwise.

References

1 K. Panplado, P. Intasri, A. Sirimungkala and T. Somboon, *ScienceAsia*, 2018, **44**, 102–108.

2 R. J. Field and A. T. Winfree, *J. Chem. Educ.*, 1979, **56**, 754.

3 A. Adamatzky, M. Tsompanas, T. C. Draper, C. Fullarton and R. Mayne, *ChemPhysChem*, 2020, **21**, 90–98.

4 R. J. Field, E. Körös and R. M. Noyes, *J. Am. Chem. Soc.*, 1972, **94**, 8649–8664.

5 M. Dueñas-Díez and J. Pérez-Mercader, *iScience*, 2019, **19**, 514–526.

6 M. Dueñas-Díez and J. Pérez-Mercader, *Front. Chem.*, 2021, **9**, 611120.

7 R. J. Field and R. M. Noyes, *J. Chem. Phys.*, 1974, **60**, 1877–1884.

8 Y. Gao and H.-D. Foersterling, *J. Phys. Chem.*, 1995, **99**, 8638–8644.